

Supporting information

Materials

Indigo (>97%) was purchased from TCI. Decamethylchromocene (Cp^*Cr , >95%) and chloro(1,5-cyclooctadiene)rhodium dimer ($\{\text{Rh}^{\text{I}}(\text{cod})\text{Cl}\}_2$, 98%) were purchased from Strem. *o*-Dichlorobenzene ($\text{C}_6\text{H}_4\text{Cl}_2$) was distilled over CaH_2 under reduced pressure; *n*-hexane was distilled over Na/benzophenone. All operations on the synthesis of **1** and their storage were carried out in a MBraun 150B-G glove box with controlled atmosphere and water and oxygen content less than 1 ppm. The solvents were degassed and stored in the glove box. KBr pellets for IR- and UV-visible-NIR measurements were prepared in the glove box. Polycrystalline sample of **1** was placed in 2 mm quartz tubes in anaerobic conditions for EPR and SQUID measurements and sealed under 10^{-5} torr pressure.

General

UV-visible-NIR spectra were measured in KBr pellets on a Perkin Elmer Lambda 1050 spectrometer in the 250-2500 nm range. FT-IR spectra ($400\text{-}7800\text{ cm}^{-1}$) were measured in KBr pellets with a Perkin-Elmer Spectrum 400 spectrometer. EPR spectra were recorded for polycrystalline samples of **1** with a JEOL JES-TE 200 X-band ESR spectrometer equipped with a JEOL ES-CT470 cryostat working between room and liquid helium temperatures. A Quantum Design MPMS-XL SQUID magnetometer was used to measure static magnetic susceptibility of **1** in 100 mT magnetic field in cooling and heating conditions in the 300 – 1.9 K range. A sample holder contribution and core temperature independent diamagnetic susceptibility (χ_{d}) were subtracted from the experimental values. The χ_{d} values were estimated by the extrapolation of the data in the high-temperature range by fitting the data with the following expression: $\chi_{\text{M}} = C/(T - \Theta) + \chi_{\text{d}}$, where C is Curie constant and Θ is Weiss temperature. Effective magnetic moment (μ_{eff}) was calculated with the following formula: $\mu_{\text{eff}} = (8 \cdot \chi_{\text{M}} \cdot T)^{1/2}$.

Synthesis

The crystals of (indigo-*O,O*)($\text{Cp}^*\text{Cr}^{\text{II}}\text{Cl}$) (**1**) were obtained by the following procedure. 14 mg of indigo (0.055 mmol) was reduced by slight excess of Cp^*Cr (18 mg, 0.056 mmol) in the presence of $\{\text{Rh}^{\text{I}}(\text{cod})\text{Cl}\}_2$ (14 mg, 0.028 mmol) in 16 mL of *o*-dichlorobenzene. At the beginning indigo completely dissolved during 10 minutes to form red solution. Intense stirring at 100°C during 4 hours resulted in the colour change from red to brown. The solution was cooled down to room temperature and filtered into the 50 mL glass tube of 1.8 cm diameter with a ground glass plug, and 30 mL of *n*-hexane was layered over the solution. The crystals were precipitated on the walls of the tube during 1 month. Then the solvent was decanted from the crystals and they were washed with *n*-hexane to yield black parallelepiped up to $0.8 \times 0.4 \times 0.4\text{ mm}^3$ in size in 56% yield. Composition of the crystals was determined from X-ray diffraction analysis on single crystals. We tested several crystals from the synthesis and all of them showed the same unit cell parameters. Therefore, they belonged to one crystal

phase. The composition of **1** was proved by elemental analysis: Anal. Calcd for $C_{26}H_{25}ClCrN_2O_2$, $M_r = 484.93$: C 64.40, H 5.17, N 5.79, Cl 7.32; Found: C 64.12, H 5.04, N 5.61, Cl 7.12. The crystals of **1** can also be obtained by a two-step reaction: the reduction of indigo by Cp^*_2Cr and the following addition of $\{Rh^I(cod)Cl\}_2$ with the formation of brown solution.

Theoretical calculations

For theoretical calculations were performed using PBE density functional method¹ and $\Lambda 2$ basis² of cc-pVTZ quality. Atomic distribution of charge and spin density was determined by the Hirschfeld method.³ All calculations were performed using the PRIRODA program package⁴ at Joint Supercomputer Center of the Russian Academy of Sciences. This approach allows geometry of **1** to be well reproduced. Mean deviation of calculated bond lengths from experimental ones is no more than 0.02 Å, for exception of the Cr-Cl bond.

The calculated structures of *trans*-indigo (a), *cis*-indigo (c) and that of the transition state (b) at their interconversion are shown in Fig. S1. According to the calculations the molecule of *cis*-indigo has nonplanar twisted structure with the dihedral N-C-C-N, C-C-C-C and O-C-C-O angles of -4.0° , -12.6° and -13.8° , respectively. That is the result of a compromise between the conjugation energy loss and steric repulsion due to short intramolecular contacts. It is interesting that flat form of *cis*-indigo (d), which is a transition state between left and right twisted *cis*-isomer, has only slightly higher energy by 0.3 kcal/mol. The transition state b has unsymmetrical structure with one pyramidal carbon atom (on the left). In this case the dihedral N-C-C-N angle is 115.6° . It should be noted that deviations from planarity of twisted *cis*-isomer are slightly larger than those observed for *cis*-indigo in complex **1** from X-ray ray data (the corresponding angles are -3.89° , -7.00° and -13.29° , respectively).

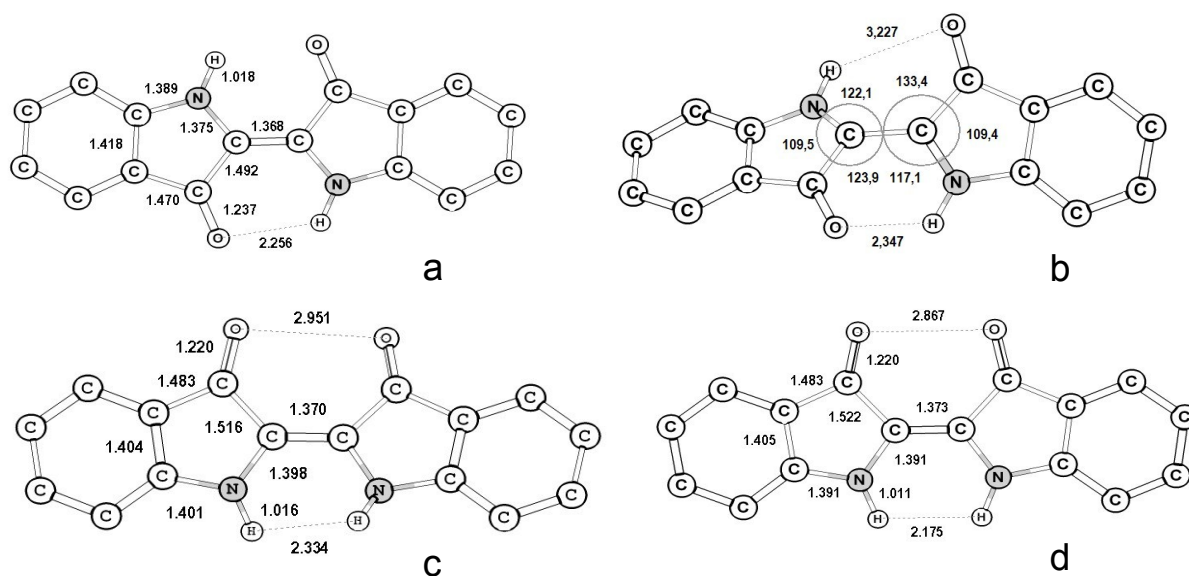


Fig. S1. Calculated structures of isomeric forms of indigo (a, c) and those of the transition states (b, d). The H atoms of the C-H bonds are omitted for clarity. Interatomic distances are given in Å and angles are given in degrees.

The energy difference between *trans*- (Fig. S2a) and *cis*- (Fig. S2c) forms of the indigo^{•-} radical anion is slightly higher by 20.6 kcal/mol than that of neutral indigo molecule (16.7 kcal/mol). The reason is stronger intermolecular H-bonds in the *cis*-isomer which are not manifested in the *trans*-isomer and stronger Coulomb repulsion leading to the elongation of the O-O distance by about 0.3 Å. Elongated C-O and central C-C bonds reflect the localization of extra electron on these fragments (75 % in total). Radical anions of *cis*-indigo have similar nonplanar structure with higher dihedral N-C-C-N, C-C-C-C and O-C-C-O angles of -7.5, -18.3 and -19.6 respectively. The transition state of conversion of *cis*- to *trans*-form has symmetric structure with smaller dihedral N-C-C-N angle of 102.2° (Fig. S2b).

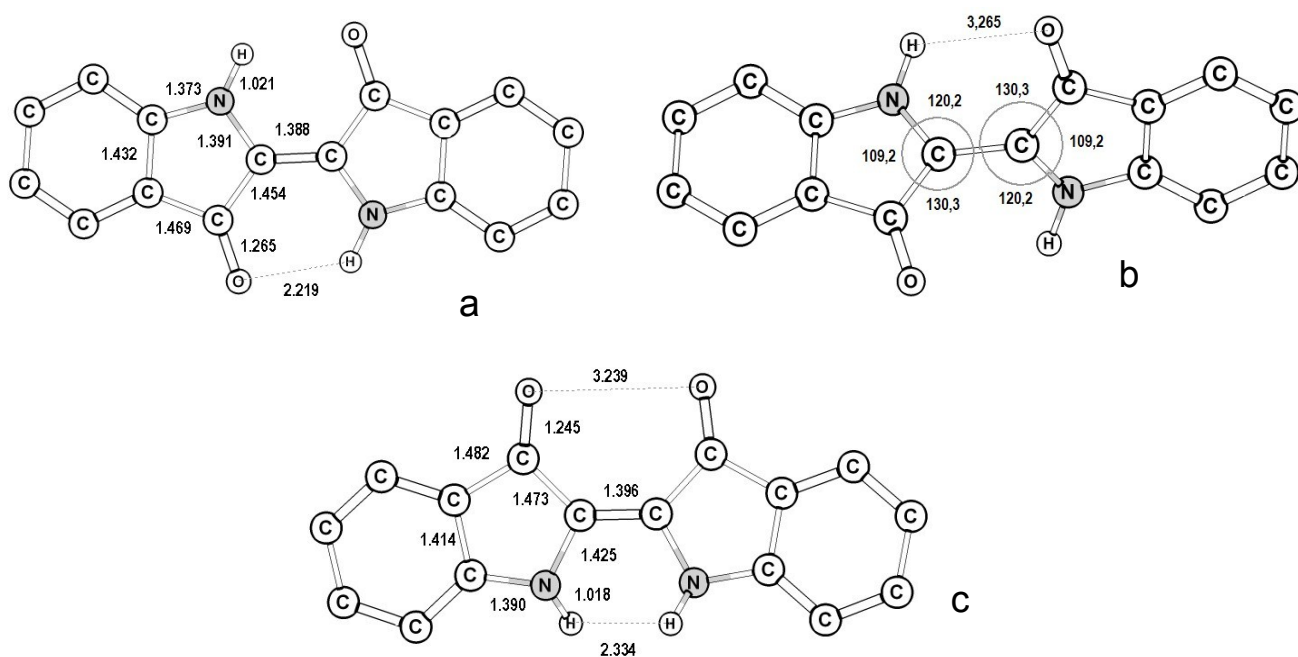


Fig. S2. Calculated structures of isomeric forms of the indigo^{•-} radical anion (a,c) and the transition state (b). The H atoms of C-H bonds are omitted for clarity. Interatomic distances are given in Å and angles are given in degrees.

The enol forms of *cis*-indigo and *cis*-indigo^{•-} have slightly higher energy by 1.1 and 2.4 kcal/mol respectively than their main *trans*-isomers. The energy barrier of *cis*-*trans* isomerization is 26.0 kcal/mol for neutral molecule and 23.2 kcal/mol for radical anion. The geometry of the transition states is shown in the Fig. S3. The dihedral N-C-C-N angles of 88.6° (a) and 89.4° (b) are close to 90°, and in both cases the carbon atoms involved in central C-C bond have planar surrounding.

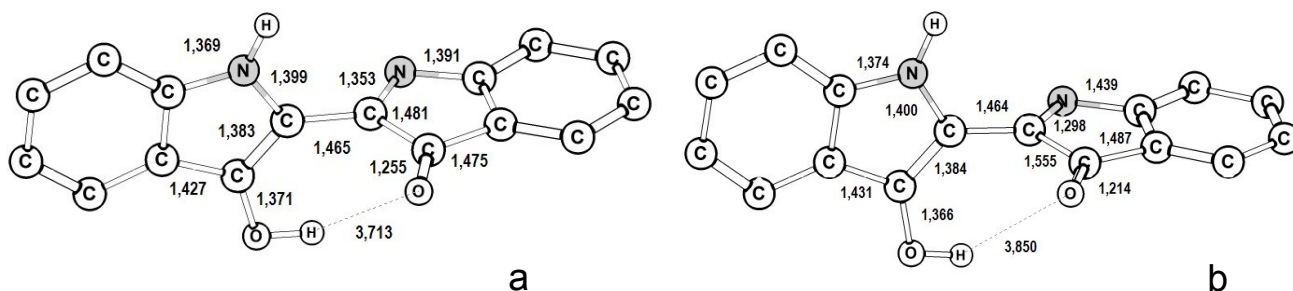


Fig. S3. Calculated structures of transition states of isomerization of enol forms of *cis*-indigo (a) and *cis*-indigo^{•-} (b). The H atoms of C-H bonds are omitted for clarity. Interatomic distances are given in Å.

The structure of the transition state of *trans-cis* isomerization of (*trans*-indigo-*O*)(Cp*₂Cr) is shown in Fig. S4. The dihedral N-C-C-N angle is 98.0°

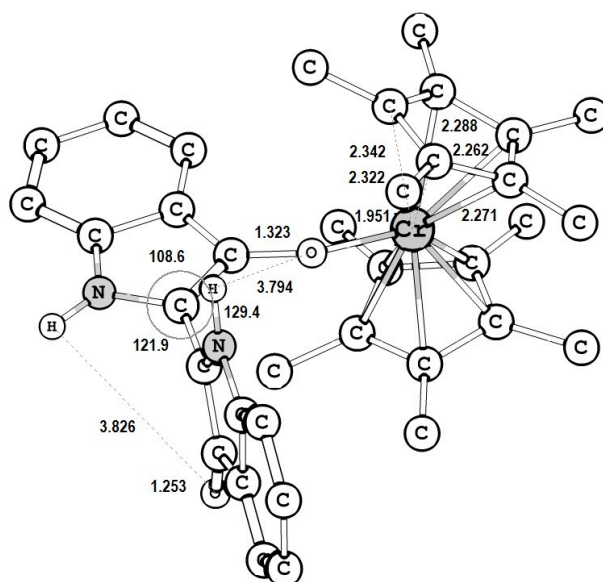


Fig. S4. Calculated structures of the transition state of *trans-cis* isomerization of (*trans*-indigo-*O*)(Cp*₂Cr). The interatomic distances are shown in Å. H atoms of C-H bonds are omitted for clarity.

X-ray crystal structure determination

Crystal data for **1**: C₂₆H₂₅ClCrN₂O₂, F.W. 484.93, black parallelepiped, 0.380×0.120×0.010 mm³; 150.0(2) K: monoclinic, space group *P*2₁/*n*, *a* = 11.7879(7), *b* = 15.2593(16), *c* = 12.5982(8) Å, β = 94.897(7)°, *V* = 2257.8(3) Å³, *Z* = 4, *d*_{calcd} = 1.427 M gm⁻³, μ = 0.651 mm⁻¹, *F*(000) = 1008, $2\theta_{max}$ = 65.390°; 26768 reflections collected, 7588 independent; *R*₁ = 0.0548 for 4721 observed data [$> 2\sigma(F)$] with 0 restraints and 294 parameters; *wR*₂ = 0.1442 (all data); final G.o.F. = 1.023. CCDC 1493779.

The intensity data for the structural analysis were collected on an Oxford diffraction "Gemini-R" CCD diffractometer with graphite monochromated MoK α radiation using an Oxford Instrument Cryojet system. Raw data reduction to F^2 was carried out using CrysAlisPro, Oxford Diffraction Ltd. The structures were solved by direct method and refined by the full-matrix least-squares method against F^2 using SHELX-2013.⁵ Non-hydrogen atoms were refined in the anisotropic approximation. Positions of hydrogen atoms were calculated geometrically.

References

1. J.P. Perdew, K. Burke, M. Ernzerhof, *Phys. Rev. Lett.* **1996**, 77, 3865-3868.
2. D.N. Laikov, *Chem. Phys. Lett.*, **2005**, 416, 116 - 120.
3. D.N. Laikov, *Chem. Phys. Lett.*, **1997**, 281, 151 - 156.
4. F. L. Hirshfeld, *Theor. Chim. Acta* **1977**, 44, 129-138.
5. G. M. Sheldrick, *Acta Cryst. Sec. A* **2008**, 64, 112-122.

IR- spectra

Table S1. IR-spectra (cm⁻¹ in KBr) of starting compounds and complex **1**.

| Components | Cp* ₂ Cr | indigo | (indigo- <i>O,O</i>)(Cp*CrCr) (1) |
|------------|---------------------|----------|---|
| Cp*CrCl | 419w | | 415w |
| | - | | 436w |
| | 585w | | 588m |
| | 1022s | | 1024w |
| | 1068w | | - |
| | 1262w | | - |
| | 1316s | | 1321s# |
| | 1375s | | 1375m# |
| | 1414w | | - |
| | 1423m | | 1429w |
| | 1448w | | - |
| | 1634m | | - |
| | 2852w | | 2852w |
| | 2899w | | 2916w |
| | 2955w | | - |
| | Indigo | | 563w |
| | | 643w | 643w |
| | | 699w | 675w |
| | | 714w | - |
| | | 745w sh | 736s |
| | | 755m | 753m |
| | | - | 772m |
| | | 859w | - |
| | | 879w | 892w |
| | | 1012w | 1006w |
| | | 1071s | - |
| | | 1096w | 1100w |
| | | 1107w | |
| | | 1129s | 1123m |
| | | 1173s | 1194m |
| | | 1200s | 1206s 1222s |
| | | 1298m | 1295m |
| | | 1318m | 1321s# |
| | | 1392m | 1375m# |
| | | 1409w sh | - |
| | | 1462s | 1461s |
| | | 1483m | 1481s 1508s |
| | | 1586w | 1585w |
| | | 1613s | 1607w |
| | | 1627s | 1615w |
| | | 3040w | - |
| | 3058w | 3058w | |
| | 3250m | 3236m | |
| | 3270m | 3295m | |

Bands are overlapped, w - weak intensity, m – middle intensity, s – strong intensity, sh – shoulder

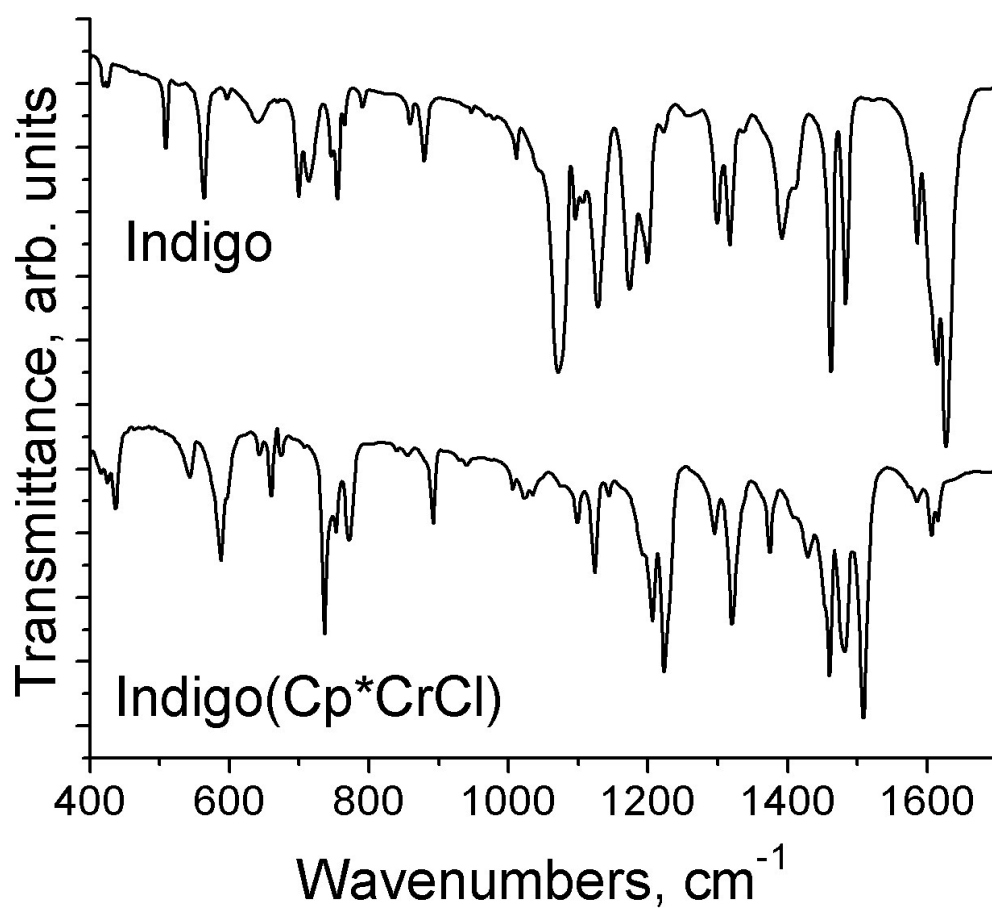


Fig. S5. IR spectrum of starting indigo and coordination complex (indigo-*O,O*)(Cp*Cr^{II}Cl) (**1**) measure in KBr pellets. Pellet of **1** was prepared in anaerobic conditions.

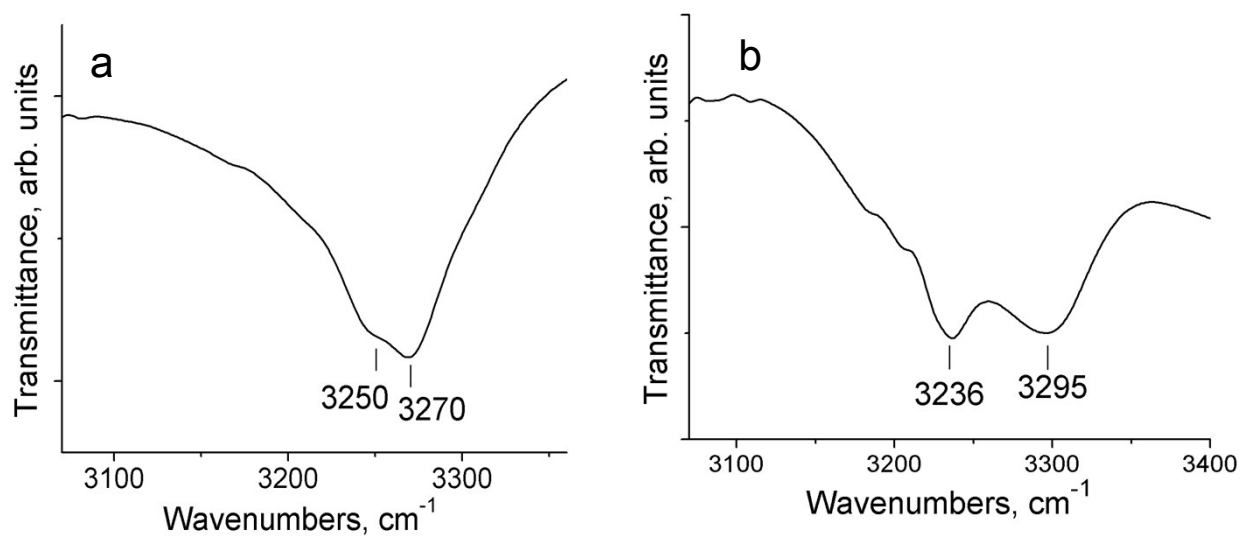


Fig. S6. IR spectra of starting indigo (a) and complex **1** (b) in the range of the N-H vibrations.

Data of magnetic measurements for complex 1.

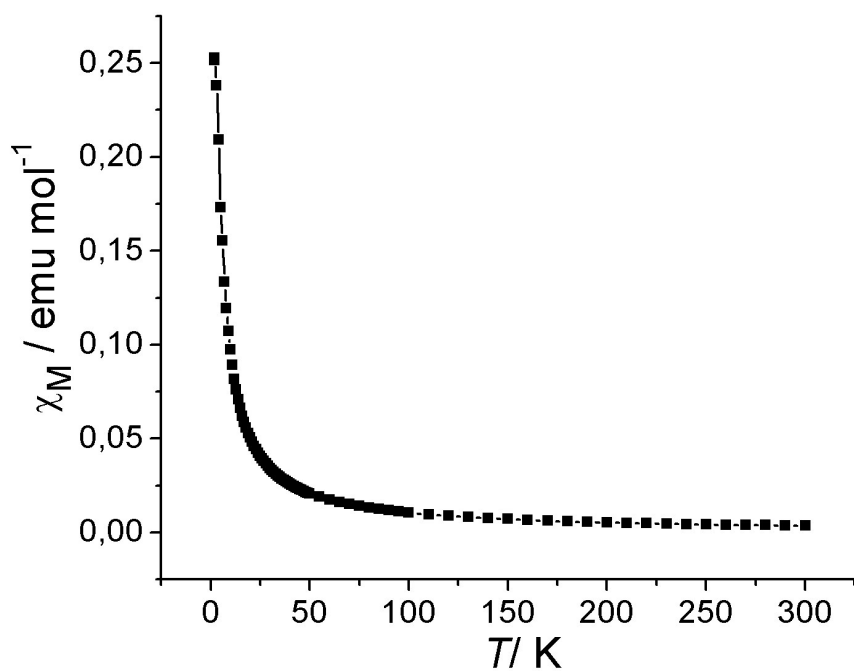


Fig. S7. Temperature dependence of molar magnetic susceptibility of polycrystalline **1** in the 1.9-300 K range.

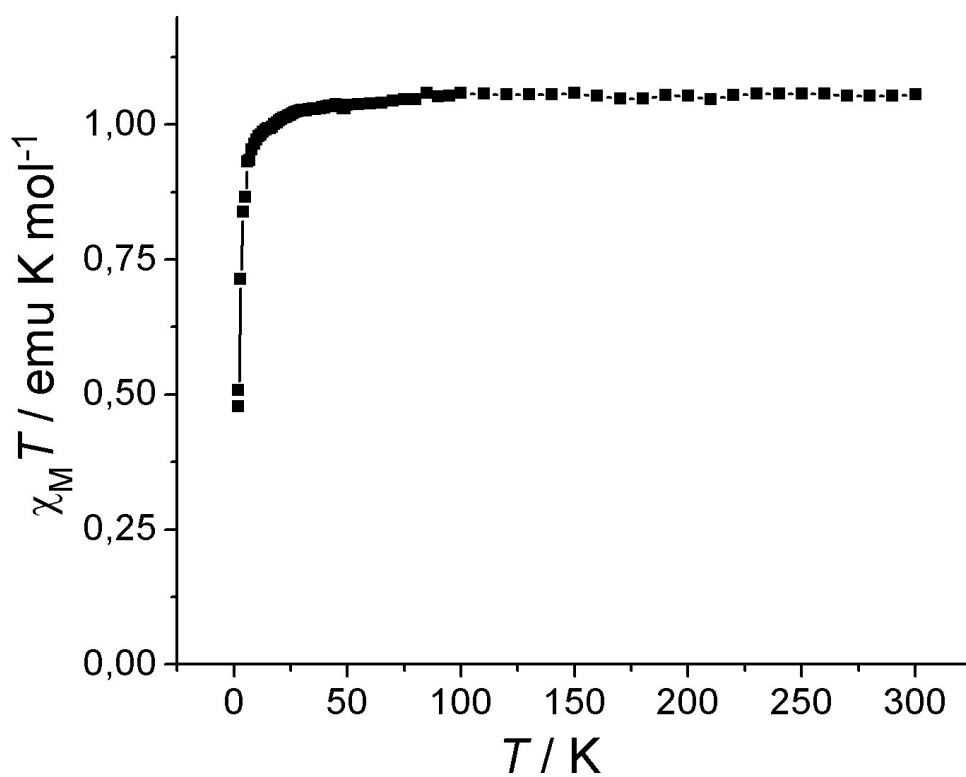


Fig. S8. Temperature dependence of the $\chi_M T$ value of polycrystalline **1** in the 1.9-300 K range.